Int. J. Heat Mass Transfer. Vol. 34, No. 6, pp. 1559–1564, 1991
Printed in Great Britain

0017–9310/91 $3.00+0.00

TECHNICAL NOTES

Transient three-dimensional natural convection in a differentially heated cubical enclosure

TORU FUSEGI,†‖ JAE MIN HYUN‡ and KUNIO KUWAHARA§

† Institute of Computational Fluid Dynamics, 1-22-3 Haramachi, Meguro, Tokyo 152, Japan
‡ Department of Mechanical Engineering, Korea Advanced Institute of Science and Technology, Chong Ryang, Seoul 131, Korea
§ Institute of Space and Astronautical Science, 3-1-1 Yoshinodai, Sagamihara, Kanagawa 229, Japan

(*Received* 21 *May* 1990 *and in final form* 31 *July* 1990)

INTRODUCTION

NATURAL convection flow analysis in enclosures has many thermal engineering applications, such as cooling of electronic devices, energy storage systems and fire-safe compartments. In the design of such devices, the transient behavior of flows is of vital interest in order to assess the maximum heat transfer rate, to cite an example. The transient flow properties may differ significantly from the steady-state values. In the present paper, a numerical study is conducted on three-dimensional transient natural convection in an air-filled cubical enclosure, which is heated differentially at its vertical side walls. As shown in Fig. 1, the entire system is initially at rest and at a uniform temperature of T_0. Suddenly, the right vertical wall of the enclosure is heated isothermally at a temperature of T_H, while the left side is cooled at a temperature of T_C. The remaining four walls are thermally insulated. The overall temperature difference, $T_H - T_C$, is set equal to one-tenth of the film temperature, $(T_C + T_H)/2$, which is used as the reference temperature, T_0, of the problem. The geometry and the initial and boundary conditions are mathematically well posed; they provide adequate models for relevant thermal engineering systems.

To the present authors' knowledge, comprehensive and thorough time-dependent three-dimensional investigations are not available in the literature. Steady-state two-dimensional numerical analyses have been carried out over an extensive range of Rayleigh numbers of $10^3 \leqslant Ra \leqslant 10^{16}$ (e.g. ref. [1]). For $10^3 \leqslant Ra \leqslant 10^6$ and a Boussinesq fluid of $Pr = 0.71$, a set of benchmark solutions for steady two-dimensional flows has been suggested [2]. Research efforts have been relatively scarce for transient two-dimensional problems [3–5]. The impact of internal gravity oscillations on the global heat transfer characteristics has been of considerable concern in such two-dimensional situations [4, 5].

In order to better simulate practical situations, three-dimensional flow calculations are highly desirable. However, solution of the three-dimensional flow equations requires far larger computational resources than that for two-dimensional calculations. Steady-state three-dimensional laminar flow has been studied for enclosures of the length aspect ratio (enclosure depth/width), A_z, varying from 2 to 4 [6, 7]. Gross features observed in the enclosures reveal highly three-dimensional structures of the flow. The enclosures with $A_z = 1$ and 2 have been considered in Lankhorst and Hoogendoorn [8], who computed steady flows for three Rayleigh numbers: $Ra = 10^6$, 4×10^8 and 10^{10}. In the last two cases, the k–ε turbulence model was employed. However, these previous steady-state calculations were executed by using relatively coarse finite difference meshes.

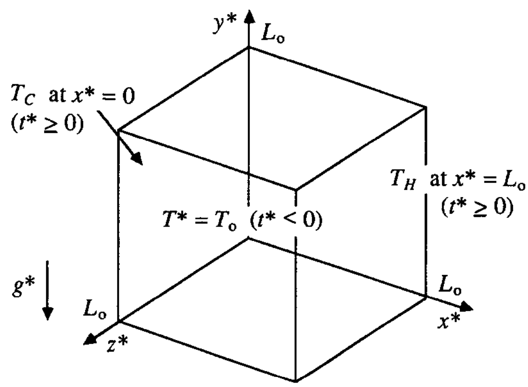

FIG. 1. The flow configuration.

In the present work, transient three-dimensional computations are carried out for a Rayleigh number of 10^6 and for $Pr = 0.71$. This is representative of high-Rayleigh number enclosure flows. An extremely fine grid network (62^3 grid points), which has been used in a recent investigation by the present authors [9], is employed. This enables us to attain sufficient resolution of the local field characteristics. The numerical resolution of the present transient computations is comparable to the maximum accuracies that have been achieved in the previous steady-state two-dimensional situations [2]. The entire enclosure constitutes the computational field. The finite difference mesh is non-uniformly distributed to handle steep gradients of the field variables near the solid surfaces.

The flow is governed by the three-dimensional, time-dependent, incompressible Navier–Stokes and energy equations. They are solved by a control-volume based finite difference procedure. The complete mathematical formulation and a detailed description of the numerical method can be found elsewhere [9], and they are not repeated here. It suffices to mention that the convective terms are discretized by the QUICK methodology modified for non-uniform grids [10] and that the iterative solution algorithm is based on the well-known SIMPLE type [11] and the Strongly Implicit Scheme [12].

The present research is a direct extension of the previous three-dimensional, steady-state analysis mentioned above. The primary objective of this study is to present complete

‖ Author to whom all correspondence should be addressed.

NOMENCLATURE

A aspect ratio (enclosure height/width)
c_p specific heat at constant pressure [J kg^{-1} K^{-1}]
g gravitational acceleration [m s^{-2}]
k thermal conductivity [W m^{-1} K^{-1}]
L_0 reference length (enclosure height) [m]
N Brunt Väisälä frequency, $[g\beta(T_H - T_C)/L_0]^{1/2}$ [s^{-1}]
$Nu_{overall}$ overall Nusselt number
Pr Prandtl number, $c_p\mu/k$
Ra Rayleigh number, $g\beta c_p \rho^2 L_0^3(T_H - T_C)/\mu k$
t non-dimensional time, t^*N
T non-dimensional temperature, T^*/T_0
T_0 reference temperature, $(T_C + T_H)/2$ [m s^{-1}]
T_C, T_H cooled and heated side wall temperatures [K]
u_0 reference convective velocity, $[g\beta L_0(T_H - T_C)]^{1/2}$ [m s^{-1}]
x, y, z non-dimensional Cartesian coordinates, $(x^*, y^*, z^*)/L_0$.

Greek symbols
β thermal expansion coefficient [K^{-1}]
μ viscosity [kg m^{-1} s^{-1}]
ρ density [kg m^{-3}]
ω non-dimensional vorticity, $\omega^* L_0/u_0$.

Superscript
$*$ dimensional quantities.

three-dimensional pictures of the gross features of time-evolving convective patterns in a cubical enclosure. At a high Rayleigh number, it is anticipated that the distinct boundary layers are present near the walls; in the bulk of the interior, a near-stagnant core will be a salient feature. The present paper clearly captures these prominent transient three-dimensional characteristics by use of the state-of-the-art computer simulation techniques. The field characteristics of the transient natural convection inside the enclosure are examined by elaborate three-dimensional numerical visualizations of the results, as have been done in the steady-state calculations [9]. Time-dependent changes in the flow characteristics and heat transfer rate in the enclosure are scrutinized, and the decay of the internal gravity waves in the enclosures is discernible.

The three-dimensional numerical results of the present study provide useful and systematic data for this fundamental flow model; examination of the data permits closer analyses of transient three-dimensional features. In particular, the quantitative information of the internal gravity oscillations will be available in the present numerical solutions.

It is stressed that the present numerical methods are designed to describe the true time-dependent process of the physical phenomena. This is in contrast to the false-time transient techniques [2], which are used to accelerate the convergence of solutions at the steady state.

RESULTS AND DISCUSSION

Time evolutions of the temperature and flow fields at $Ra = 10^6$ are examined by using three-dimensional perspective views of the isotherms and the absolute values of the vorticity. The vorticity, ω, derivable from the velocity field, is a direct indicator of the gradients of the flow.

Initially, the fluid is at a uniform temperature of T_0 and motionless. A sudden differential heating at $t \geqslant 0$ at the two vertical side walls ($x = 0$ and 1) creates sharp temperature gradients in the proximity of the isothermal walls. In the central region of the enclosure, the fluid is still at the initial uniform temperature; thus, the heated fluid near the side wall at $x = 1$ starts to rise, and the cooled fluid near $x = 0$ moves downward. Subsequent to this initial development, the heated and cooled fluids flow along the ceiling and floor of the enclosure, respectively, in opposite directions. After some time, these flows meet each other near the corners of the horizontal walls. The flow field at this stage is sketched in Fig. 2(a), which depicts the temperature and flow fields at $t = 7.5$. Near the end walls ($z = 0$ and 1), the isotherms adjacent to the horizontal walls ($y = 0$ and 1) develop z-variations. This is due to the no-slip conditions imposed on the end walls. Consequently, vorticity is generated in these wall regions.

After the fluid layers merge, *piling-up* of the fluids in the corner areas between the side walls and horizontal walls takes place as expounded by Patterson and Imberger [4] for two-dimensional situations. This increases the overall temperature gradients in the regions in the vicinity of the isothermal walls. In the interior regions, the thermal field begins to stratify, as demonstrated in Fig. 2(b). The vorticity field illustrates that the intense flow motion is now mostly confined into the thin layers in the proximity of the vertical isothermal walls, in conjunction with the formation of the stratified structure in the interior.

As time progresses, the thermal stratification is substantially accomplished, with the resulting near-stagnant interior core. As the steady state is approached (see Fig. 2(c)), the global field is well characterized by a combined structure of the boundary layers near the walls and the near-stagnant interior core.

The time evolutions of the fields portrayed above are qualitatively consistent with those described in Küblbeck *et al.* [3], who considered a two-dimensional square enclosure at lower Ra/Pr values of around 10^4.

In an effort to portray in further detail the time-dependent flow process, Fig. 3 plots the exemplary behavior of the local Nusselt number, Nu_{local}, at the heated wall ($x = 1$). Its definition is given as

$$Nu_{local} = -\partial T(1, y, z)/\partial x. \quad (1)$$

It is noted that the behavior of Nu_{local} is quite insensitive to the z locations in the bulk of the enclosure. At small times (e.g. at $t = 7.5$), the y-variations of the local Nusselt number are rather mild. At later times, large changes of Nu_{local} are noticed in the regions close to the bottom wall ($y = 0$). When the steady state is reached, the peaks of the local Nusselt number are seen slightly away from the bottom plane. It is evident that the differences in the Nusselt number profiles at $z = 0.2$ and 0.5 are very minor; this points to the prior assertion that the two-dimensionality of the heat transfer characteristics is largely applicable in these central portions of the enclosure.

Next, the time evolution of the heat transfer rate is scrutinized by using the overall Nusselt number, $Nu_{overall}$, which is calculated as

$$Nu_{overall} = \int_0^1 \int_0^1 \left[-\frac{\partial T}{\partial x}(x = a, y, z) + \sqrt{(Ra\,Pr)}\,u(T(x = a, y, z) - 1) \right] \mathrm{d}y\,\mathrm{d}z \quad (2)$$

where the terms in brackets represent the local Nusselt number. Figure 4 illustrates the time histories of $Nu_{overall}$ at the enclosure mid-plane ($x = 0.5$) and at the heated wall

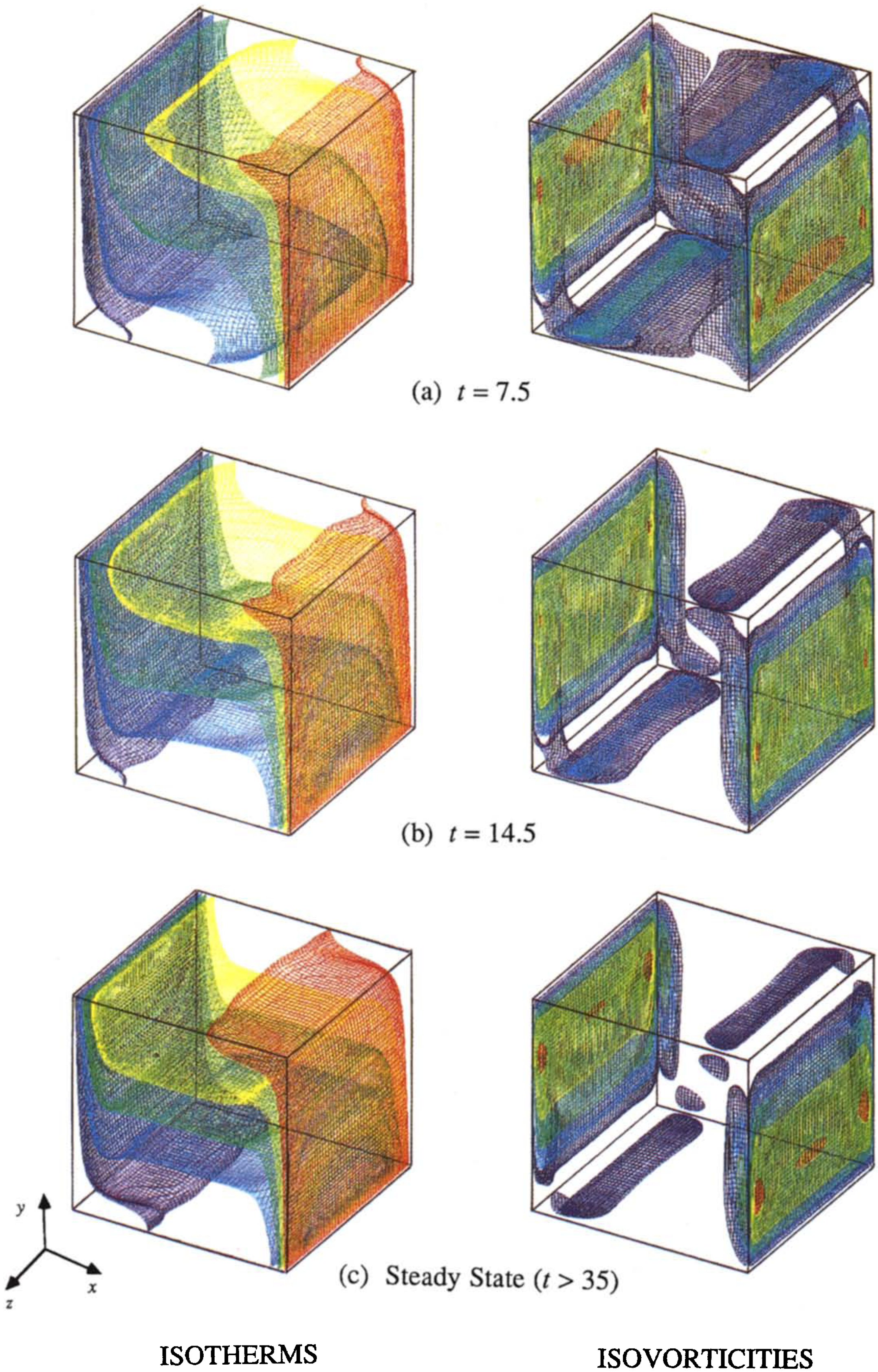

FIG. 2. Evolutions of the temperature and the absolute vorticity fields (contour levels: (for isotherms) 0.9667 (purple), 0.9833 (blue), 1.0 (green), 1.017 (yellow), 1.033 (red); (for isovorticity surfaces) 3.6 (purple), 7.2 (blue), 10.8 (green), 14.4 (yellow), 18.0 (red)).

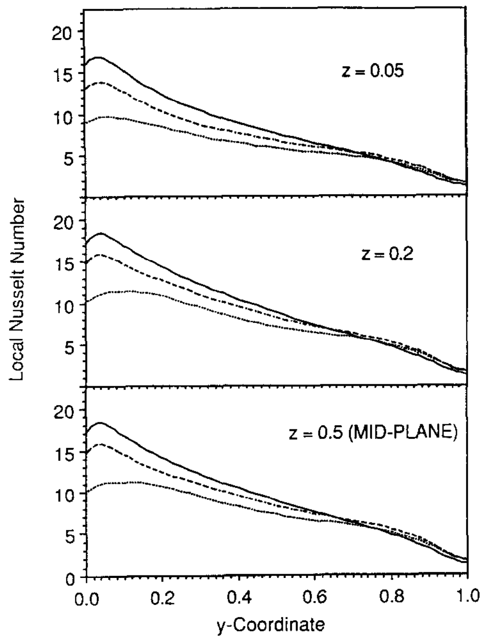

FIG. 3. Time-dependent variations of the local Nusselt number at the heated wall ($x = 1$) (·····, $t = 7.5$; -----, $t = 14.5$; ——, steady state).

($x = 1$). The Nusselt number at $x = 1$ takes very large values initially due to the sudden heating, and decreases rapidly to reach a local minimum. It increases gradually afterward, in a generally monotonic manner, until the steady state is approached. The behavior of the Nusselt number in the interior core, as typified in the curve for $x = 0.5$ in Fig. 4, is strikingly different from that at the solid side wall. The temperature in the interior core does not respond immediately to the changes in the boundary walls. As was succinctly espoused in two-dimensional simulations [13–15], the temperature at an interior location remains unchanged, maintaining the original uniform value, T_0, until the arrival of the *temperature front* [13–15]. The temperature front in the interior propagates vertically during the transient phase, separating the region of uniform temperature and the stratified region. Figure 4 clearly illustrates the advent of this

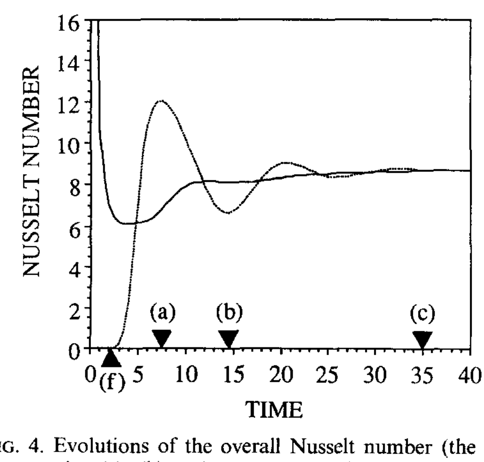

FIG. 4. Evolutions of the overall Nusselt number (the time instants, i.e. (a), (b) and (c), correspond to those shown in Fig. 2 (——, at the heated wall ($x = 1$); ······, in the mid-plane ($x = 0.5$)).

temperature front, see (f) in the figure. Accordingly, no convective heat transfer is discernible in the curve for $x = 0.5$ during the early phase of the transient process, i.e. the time segment from $t = 0$ and (f).

Soon after the temperature front passes through the interior location under consideration, the convective flow processes become vigorous. These convective activities, coupled with the steep temperature gradients, give rise to highly enhanced heat transfer. Accordingly, the overall Nusselt number demonstrates rapid increases with time around $t =$ (a).

As time elapses further, the temperature field in the interior tends toward the vertically-linear distribution, as can be inferred from Fig. 2(c). In the large-time steady-state limit, the interior of the entire enclosure supports an almost linear vertical temperature profile; the Nusselt number averaged over each plane of $x =$ constant attains the same constant value (8.77) in the whole of the enclosure interior.

Another significant feature of the temporal behavior of the Nusselt number in the interior is the pronounced oscillations superposed on the general approach to the steady state. The basic mechanism for this oscillatory nature was delineated [4]. By the way of physically insightful scaling arguments, Patterson and Imberger [4] stressed that these oscillations are reflective of the presence of internal gravity waves. Stemming from elaborate scaling analyses for a two-dimensional enclosure, Patterson and Imberger [4] and Patterson [16] suggested a criterion for the existence of such oscillations

$$Ra > Pr^4 A^{-4}. \tag{3}$$

The above criterion has been the subject of verification by several two-dimensional studies (e.g. refs. [5, 16, 17]) that covered broad ranges of the Rayleigh and Prandtl numbers. The present calculations clearly point to the existence of such oscillations in the three-dimensional situations. Furthermore, the period of oscillations is approximately 12.0, as detected in Fig. 4. There are no published data for the oscillation period for the *three-dimensional* flows in the parameter ranges considered in this note; however, the period of oscillations for *two-dimensional* enclosure flows has been estimated [4] as

$$\tau = 2\pi(1+A^2)^{1/2}. \tag{4}$$

This two-dimensional analytical prediction for the aspect ratio $A = 1$ gives $\tau = 8.89$. These comparisons indicate that the detected period of oscillations in Fig. 4 is at least of the same order of magnitude as that of the two-dimensional analytical estimate. The oscillations in Fig. 4 die out with time after approximately three cycles; this is due to the effects of viscosity, as remarked by the prior authors [4, 5, 13].

SUMMARY

Transient three-dimensional natural convection in a differentially heated cubical enclosure is studied numerically at a representative high-Rayleigh number of 10^6. By employing a fine grid network, high-resolution computed fields have been secured. The present resolution is comparable to the best of the previous steady-state two-dimensional analyses. Time evolutions of the temperature and flow fields are illustrated by the development of the distinct boundary layers along the isothermal walls and the near-stagnant interior core. The behavior of the heat transfer rate in the enclosure is seen to be considerably influenced by the presence of the internal gravity wave motion. The period of the oscillations appears to be of the same order of magnitude as the analytical prediction of two-dimensional flows.

Note: the interested readers should contact the first author for the quantitative results of these three-dimensional computations.

REFERENCES

1. N. C. Markatos and K. A. Pericleous, Laminar and turbulent natural convection in an enclosed cavity, *Int. J. Heat Mass Transfer* **27**, 755–772 (1984).
2. G. de Vahl Davis, Natural convection of air in a square cavity: a bench mark numerical solution, *Int. J. Numer. Meth. Fluids* **3**, 249–264 (1983).
3. K. Küblbeck, G. P. Merker and J. Straub, Advanced numerical computation of two-dimensional time-dependent free convection in cavities, *Int. J. Heat Mass Transfer* **23**, 203–217 (1980).
4. J. Patterson and J. Imberger, Unsteady natural convection in a rectangular cavity, *J. Fluid Mech.* **100**, 65–86 (1980).
5. J. M. Hyun and J. W. Lee, Numerical solutions for transient natural convection in a square cavity with different sidewall temperatures, *Int. J. Heat Fluid Flow* **10**, 146–151 (1989).
6. G. D. Mallinson and G. de Vahl Davis, Three-dimensional natural convection in a box: a numerical study, *J. Fluid Mech.* **83**, 1–31 (1977).
7. T. S. Lee, G. H. Son and J. S. Lee, Numerical predictions of three-dimensional natural convection in a box, *Proc. 1st KSME–JSME Thermal and Fluids Engng Conf.*, Vol. 2, pp. 278–283 (1988).
8. A. M. Lankhorst and C. J. Hoogendoorn, Three-dimensional numerical calculations of high Rayleigh number natural convective flows in enclosed cavities, *Proc. 1988 Natn. Heat Transfer Conf.*, ASME HTD-96, Vol. 3, pp. 463–470 (1988).
9. T. Fusegi, J. M. Hyun, K. Kuwahara and B. Farouk, A numerical study of three-dimensional natural convection in a differentially heated cubical enclosure, *Int. J. Heat Mass Transfer* **34**, 1543–1557 (1991).
10. C. J. Freitas, R. L. Street, A. N. Findikakis and J. R. Koseff, Numerical simulation of three-dimensional flow in a cavity, *Int. J. Numer. Meth. Fluids* **5**, 561–575 (1985).
11. S. V. Patankar, *Numerical Heat Transfer and Fluid Flow*, Chap. 6. Hemisphere, Washington, DC (1980).
12. H. L. Stone, Iterative solution of implicit approximations of multi-dimensional partial differential equations, *J. Numer. Analysis* **5**, 530–558 (1968).
13. L. Rahm and G. Walin, On thermal convection in stratified fluids, *Geophys. Astrophys. Fluid Dyn.* **13**, 51–65 (1979).
14. J. M. Hyun, Transient process of thermally stratifying an initially homogeneous fluid in an enclosure, *Int. J. Heat Mass Transfer* **27**, 1936–1938 (1984).
15. J. M. Hyun, Thermally-forced stratification build-up in an initially isothermal contained fluid, *J. Phys. Soc. Japan* **54**, 942–949 (1985).
16. J. C. Patterson, On the existence of an oscillatory approach to steady natural convection in cavities, *J. Heat Transfer* **106**, 104–108 (1984).
17. R. Yewell, D. Poulikakos and A. Bejan, Transient natural convection experiments in shallow enclosures, *J. Heat Transfer* **104**, 533–538 (1982).

Int. J. Heat Mass Transfer. Vol. 34, No. 6, pp. 1564–1567, 1991
Printed in Great Britain

0017-9310/91 $3.00 + 0.00

Some exact solutions for free convective flows over heated semi-infinite surfaces in porous media

D. A. S. Rees† and A. P. Bassom

Department of Mathematics, North Park Road, University of Exeter, Exeter, Devon EX4 4QE, U.K.

(*Received* 13 *June* 1990 *and in final form* 9 *August* 1990)

1. INTRODUCTION

THE STUDY of convection generated by a heated semi-infinite surface embedded in a saturated porous medium has attracted extensive treatment in recent years. Of main concern has been the practical need to determine accurately the heat transferred into the porous medium from heated surfaces of various orientations. After the pioneering work of Cheng and Minkowycz [1] and Cheng and Chang [2], who considered flows generated by vertical and upward-facing horizontal surfaces, respectively, attention has been focused on higher order analyses (see refs. [3–6]). Detailed reviews of much of this work are given in Cheng [7] and Tien and Vafai [8]. However, the accuracy of high order analyses is limited due to the appearance of eigensolutions at some point in the expansion. This is due to the asymptotic nature of the analysis and a lack of precise knowledge of the effects of the leading edge. But we note in passing that a recent paper by Pop *et al.* [9] has sought to account for the 'leading-edge effect' by means of a deformed streamwise coordinate.

In this note we reconsider two of the more well-researched configurations. We consider a wedge-shaped region of saturated porous medium bounded by two semi-infinite surfaces, one heated isothermally, the other insulated. In particular, we study the two cases: (i) a vertical heated surface with a wedge angle of π, and (ii) a horizontal upward-facing surface with a wedge angle of $3\pi/2$. It is shown that, for these configurations, the full non-linear governing equations reduce to a set of ordinary differential equations upon introduction of appropriate coordinate transformations. These ODEs are, in fact, identical to those describing the classical leading order boundary layer profiles, and therefore detailed descriptions of the flow and temperature fields in the neighbourhood of the leading edge are determined, as are expressions for the heat transferred into the medium.

2. STATEMENT OF THE PROBLEM

The configuration we consider is as described above and shown in ref. [6]. The surface $y = 0$, $x > 0$ is held at a non-dimensional temperature of unity whilst the ambient temperature of the saturated medium is zero (see ref. [6] for details of the nondimensionalization). Assuming that Darcy's law and the Boussinesq approximation are both valid, the two-dimensional equations become

$$\psi_{xx}+\psi_{yy} = (\cos\delta)\theta_y - (\sin\delta)\theta_x \tag{1a}$$

$$\theta_{xx}+\theta_{yy} = \psi_y\theta_x - \psi_x\theta_y . \tag{1b}$$

Since there is no natural length scale in the problem the Rayleigh number can be considered either to have been

† Permanent address: School of Mechanical Engineering, University of Bath, Claverton Down, Bath BA2 7AY, U.K.